arXiv:cond-mat/9909340v1 [cond-mat.mes-hall] 23 Sep 1999

In-plane gate single-electron transistor in Ga[Al]As fabricated by scanning probe lithography

S. Lüscher, A. Fuhrer, R. Held, T. Heinzel, and K. Ensslin
Solid State Physics Laboratory, ETH Zürich, CH-8093 Zürich, Switzerland

W. Wegscheider *+
* *Walter Schottky Institut, TU München, 85748 Garching, Germany*
+ *Institut für Angewandte und Experimentelle Physik, Universiät Regensburg, 93040 Regensburg, Germany*

A single-electron transistor has been realized in a Ga[Al]As heterostructure by oxidizing lines in the GaAs cap layer with an atomic force microscope. The oxide lines define the boundaries of the quantum dot, the in-plane gate electrodes, and the contacts of the dot to source and drain. Both the number of electrons in the dot as well as its coupling to the leads can be tuned with an additional, homogeneous top gate electrode. Pronounced Coulomb blockade oscillations are observed as a function of voltages applied to different gates. We find that, for positive top-gate voltages, the lithographic pattern is transferred with high accuracy to the electron gas. Furthermore, the dot shape does not change significantly when in-plane voltages are tuned.

Single electron transistors (SETs) [1] are currently the subject of intense research activities. They can be used as devices which rely on the discreteness of the electron charge, for example highly sensitive electrometers [2–5], or single electron pumps as a possible current standard [6]. Furthermore, SETs defined in a two-dimensional electron gas (2DEG) of a semiconductor heterostructure are also known as "quantum dots", and can be seen as tunable artificial atoms with interacting electrons. The interplay between Coulomb interactions and quantum size effects has been widely studied in such structures. [7]

Generally speaking, an SET consists of a conducting island, which is weakly coupled to two reservoirs via tunnel barriers. In order to be able to tune the electrochemical potential of this island, a nearby gate electrode is coupled capacitively to it. In recent years, a variety of fabrication methods for tunable semiconductor quantum dots has been reported, each having its particular strengths and weaknesses. The most common scheme consists of patterning metallic top gate electrodes by electron beam lithography. [7] By applying negative voltages to these gates, the quantum dot is induced in the electron gas. Its shape and electron density as well as its coupling to the leads can be tuned over wide ranges. The disadvantage of this method is that due to the large lateral depletion lengths of the order of 100nm, the dot shape deviates significantly from the top gate pattern. Furthermore, changing the number of electrons inside the dot changes its shape as well, which is reflected experimentally in gate-voltage dependent capacitances. Patterning the dot and in-plane gate electrodes by wet chemical etching results in quite similar advantages and disadvantages. [8,9] Other schemes of fabricating quantum dots are focused laser beam-induced doping, [10] and focused Ga ion beam implantation in combination with top gates [11]. Here, the lateral depletion is smaller. However, it is known that scattering at edges defined by such implantation techniques is highly diffusive, [12] thus reducing, or even destroying, ballistic transport through the dot.

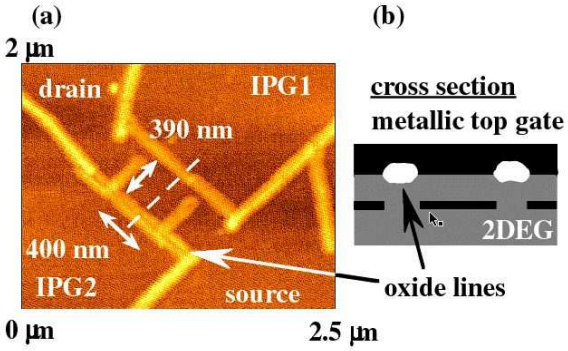

FIG. 1. Fig. 1: (a): Scanning force micrograph of the oxide pattern that defines the quantum dot, which is coupled to source and drain via small gaps in the oxide lines. The dot potential can be tuned using the electrodes IPG1 or IPG2. The picture shows the sample before the top gate metallization. The dashed line indicates the line of the cross section scheme in (b). The oxide lines deplete the electron gas underneath and separate the dot from IPG1 and IPG2. The sample is homogeneously covered by a Ti/Au top gate.

Here, we report the realization of quantum dots in a $GaAs-Al_xGa_{1-x}As$ (x=0.3) heterostructure by local oxidation of the semiconductor surface with an atomic force microscope (AFM). [13] Clear Coulomb blockade of the electron transport is observed. It is demonstrated that by combining top gates with in-plane gates, the lithographic shape of the dot can be transferred into the electron gas with high accuracy. Furthermore, by applying voltages to the in-plane gates, the occupation number of the dot can be tuned over wide ranges by leaving its shape basically unchanged.
The 2DEG in our samples is located $34nm$ below the surface. It has a sheet density of $5.0 \cdot 10^{15} m^{-2}$ and a mobility of $92 m^2/Vs$ at a temperature of T=0.1 K. The

coarse lateral structure of the sample is pre-patterned by optical lithography. A Hall bar is defined by wet chemical etching, and Ni-AuGe Ohmic contacts are alloyed into the heterostructure. Then, the dot is defined by local oxidation (LO) of the GaAs cap layer (Fig. 1a). Oxide lines (typical width 100nm and height 8nm, respectively) deplete the electron gas underneath [13], separate the quantum dot from the in-plane gates (IPG1 and IPG2) and define the connections to source and drain. In a final fabrication step, the sample is covered with a homogeneous layer of 100nm Au on top of 5nm Ti, acting as a top gate (Fig. 1b). Recently, Sasa et al. [14] reported the observation of Coulomb blockade in a quantum dot defined by combining LO on InAs/AlGaSb heterostructures with a selective wet chemical etching technique. Our technique, which works in Ga[Al]As, does not need an etch step and can be combined with additional top gates, which may be laterally patterned.

DC conductance measurements have been carried out in a $^3He/^4He$ dilution refrigerator with a base temperature of 50mK. No leakage currents ($I \leq 1pA$) between top gate and 2DEG could be detected for top gate voltages $-2V \leq V_{tg} \leq +1V$. The depleted regions under the oxide lines have typical breakdown voltages of $\pm 400mV$ which, however, depend on V_{tg}. [15] Applying voltages to the top gate changes not only the occupation number of the dot, but also its coupling to the leads. We have studied two different realizations of such quantum dots. In type 1, the dot is separated from source and drain via two highly insulating tunnel barriers when the top gate is grounded. The tunnel barriers are defined by a gap of about $20nm$ in the two oxide lines that separate the dot from source and drain. By applying positive voltages to the top gate, the tunnel barriers can be opened. In type 2, the dot is coupled to source and drain via open quantum point contacts when the top gate is grounded. This is achieved by keeping the gaps in the oxide lines at $\approx 50nm$ (Fig. 1a). Here, negative top gate voltages close the quantum point contacts.

In Fig. 2, conductance measurements on a type 1 dot are shown. Using a bias voltage of $20\mu V$, a current through the dot can be detected for $V_{tg} \geq 360mV$, and Coulomb blockade oscillations as a function of V_{tg} can be observed for $380mV \leq V_{tg} \leq 400mV$ (Fig. 2a). An average peak separation of $\Delta V_{tg} = 240\mu V$ is found, corresponding to a capacitance between top gate and dot C_{dt} of $670aF$. We modeled C_{dt} by a parallel plate capacitor. Using the distance between top gate and the 2DEG as the separation between the plates, and a dielectric constant of $\epsilon = 13$, we find an electronic dot area of $2 \cdot 10^5 nm^2$, which indicates that the lateral depletion length is clearly less than $20nm$ at the oxide lines, if about $400mV$ are applied to the top gate. This is in agreement with our earlier investigations on the depletion lengths of nanostructures defined by local oxidation. [15] Hence, the size and shape of our quantum dot resemble much more closely the lithographic pattern than that defined solely by top gates (like in conventional split-gate structures) do.

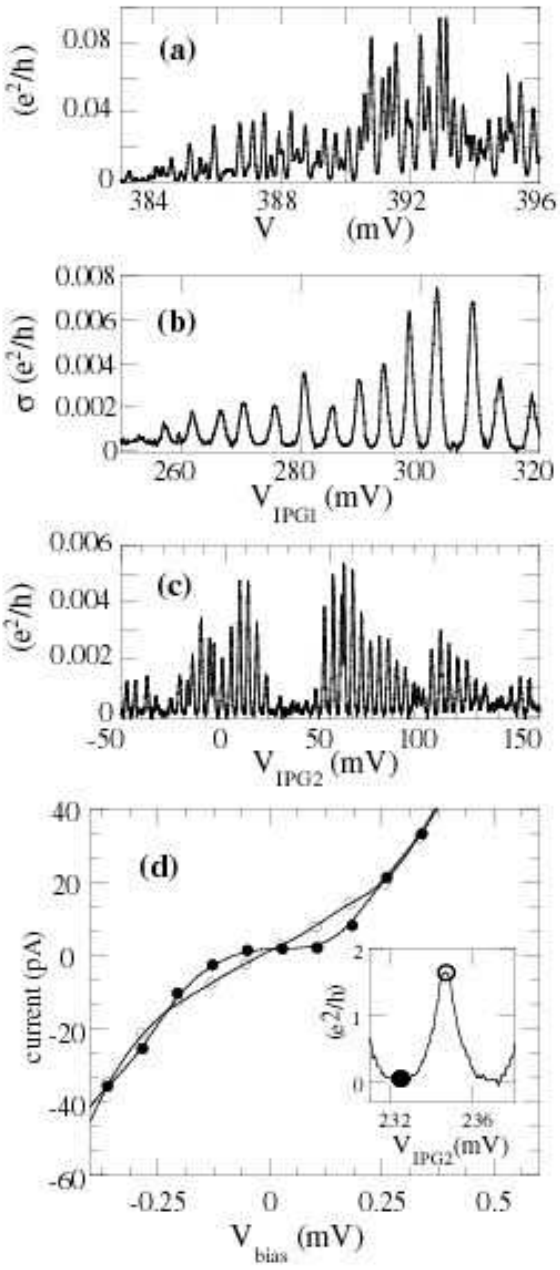

FIG. 2. Fig. 2: Conductance σ through the type 1 dot as a function of the top gate voltage (a), the voltage applied to IPG1 (b) and IPG2 (c). The temperature was $T = 120mK$ (d): I-V trace in the peak (open circles) and in the valley (full circles) of the Coulomb resonance. The inset shows the Coulomb peak used for the I-Vs.

The tuning range for IPG2 corresponds to about 100 electrons (Fig. 2c), while the tuning range of IPG1 is only about 20 electrons (Fig. 2b), which reflects the different influence of these gates on the tunnel barriers. From the average conductance peak separation as a function of the in-plane gate voltages, we determine the capacitances

for IPG1 and IPG2 to be $33aF$ and $39aF$, respectively. With a 3-dimensional numerical capacitance simulation we find excellent agreement between theoretical and experimental values of the capacitances of the dot to all three gates [16].
In Fig. 2d, I-V traces for two different IPG2 voltages are shown. The trace with the full circles, taken in the valley of a Coulomb oscillation, shows a clear Coulomb gap. From a set of I-V measurements over several Coulomb oscillation periods, we find a Coulomb gap of $410\mu eV$.

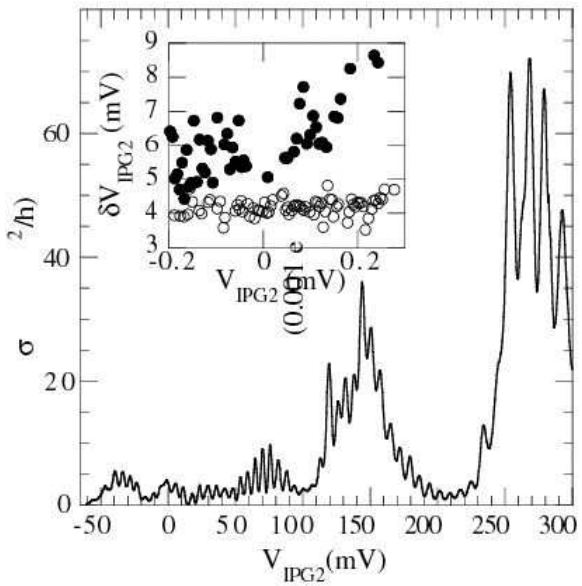

FIG. 3. Fig. 3: Conductance σ through the type 2 dot. Superimposed to the Coulomb oscillations, transmission resonances are observed. In the inset we plot the periods of the conductance oscillations δV_g as a function of V_{IPG2} obtained for the different dot types. The open circles represent the period of the peaks in the type 1 dot, which remains almost constant over the whole voltage range. For comparison, the periods in V_{IPG2}, measured in a dot of type 2, i.e. under negative top gate voltages, are represented by the full circles. Here, the period increases significantly with increasing V_{IPG2}, since the capacitance between dot and gate changes.

In Fig. 3, we show the conductance through the type 2 dot. In addition to the Coulomb oscillations, one observes well-known superimposed transmission resonances. [17] In the case of this open dot, we have to apply $V_{tg} = -130mV$ in order to close the quantum point contacts. It is obvious that, in this case, the Coulomb period increases with V_{IPG2}. In contrast, we observe in the type 1 dot, where we apply a positive top gate voltage, an approximately constant period of about $4mV$ over wide ranges of V_{IPG2}. This different behavior is visualized in the inset of Fig. 3, where the Coulomb peak separation as a function of V_{IPG2} for both dot types is shown. We interpret the constant peak separation in the type 1 dot (open circles) as a consequence of the huge carrier density due to the positive top gate voltage. Therefore, the electric fields from the in-plane gates are screened very effectively and the dot keeps its shape over the whole V_{IPG2} range. This is not the case in the type 2 dot (full circles), where a negative top gate voltage is applied, which reduces the electron density in the system.
High quality SETs can be fabricated by a variety of methods. Our approach leads to quantum dots that are highly tunable by in-plane as well as by top gate electrodes. Furthermore the substrate as well as the electrodes can be patterned by scanning probe lithography in two consecutive steps since overlay accuracy is not a critical issue with an AFM. In particular we expect to be able to realize dots containing few electrons where the charge and spin degrees of freedom can be controlled with high accuracy.
In summary, we have shown that sub-micron size quantum dots can be patterned in Ga[Al]As heterostructures by combining local oxidation of the semiconductor surface with additional top gates, and Coulomb blockade can be observed. Operating the quantum dots with positive top gate voltages results in excellent transfer of the lithographic pattern into the electron gas. In addition, the dot keeps its shape while it is tuned by in-plane gates. Hence, our fabrication scheme is highly flexible and well suited for performing experiments in which the energy spectrum of quantum dots is studied.
We wish to thank M. Bichler for growing the samples and G. Salis for his help with the sample preparation. Financial support from the Schweizerischer Nationalfonds is gratefully acknowledged.

[1] For a review, see Single Charge Tunneling, edited by H. Grabert and M. H. Devoret (Plenum, New York1992)
[2] P. Lafarge, H. Pothier, E.R. Williams, D. Esteve, C. Urbina, and M.H. Devoret, Z. Phys. B **85**, 327 (1991).
[3] M.J. Yoo, T.A. Fulton, H.F. Hess, R.L. Willett, L.N. Dunkelberger, R.J. Chichester, L.N. Pfeiffer, and K.W. West, Science **276**, 579 (1997).
[4] Y.Y. Wei, J. Weis, K.v. Klitzing, and K. Eberl, Appl. Phys. Lett. **71**, 2514 (1997).
[5] M. Koltonyuk, D. Berman, N.B. Zhitenev, R.C. Ashoori, L.N. Pfeiffer, and K.W. West, Appl. Phys. Lett. **74**, 555 (1999).
[6] J.M. Martinis, M. Nahum, and H.D. Jensen, Phys. Rev. Lett. **72**, 904 (1994).
[7] For a review, see L.P. Kouwenhoven, C.M. Marcus, P.L. McEuen, S. Tarucha, R.M. Westervelt, and N.S. Wingreen, "Electron Transport in Quantum Dots", in Mesoscopic Electron Transport, Proceedings of a NATO Advanced Study Institute, edited by L.P. Kouwenhoven, G. Schön and L. L. Sohn, (Kluwer, Dodrecht, Nether-

lands, 1997), ser. E, vol. 345, pp. 105-214.
[8] H. Pothier, J. Weis, R.J. Haug, K. v. Klitzing, and K. Ploog, Appl. Phys. Lett. **62**, 3174 (1993).
[9] T. H. Wang and S. Tarucha, Appl. Phys. Lett. **69**, 406 (1996).
[10] P. Baumgartner, W. Wegscheider, M. Bichler, G. Schedelbeck, R. Neumann, and G. Abstreiter, Appl. Phys. Lett. **70**, 2135 (1997).
[11] T. Fujisawa and S. Tarucha, Appl. Phys. Lett. **68**, 526 (1996).
[12] T. J. Thornton, M. L. Roukes, A. Scherer, and B. P. Van de Gaag, Phys. Rev. Lett. **63**, 2128 (1989).
[13] R. Held, T. Vancura, T. Heinzel, K. Ensslin, M. Holland and W. Wegscheider, Appl. Phys. Lett. **73**, 262 (1998).
[14] S. Sasa, T. Ikeda, K. Anjiki, and M. Inoue, Jpn. J. Appl. Phys. **38**, 480 (1999).
[15] R. Held, S. Lüscher, T. Heinzel, K. Ensslin and W. Wegscheider, Appl. Phys. Lett. **75**, 1134 (1999).
[16] The simulation program can be downloaded from: ftp://rle-vlsi.mit.edu/pub/fastcap/
[17] T. Heinzel, S. Manus, D.A. Wharam, J.P. Kotthaus, G. Böhm, W. Klein, G. Tränkle, and G. Weimann, Europhys. Lett. **26**, 689 (1994).